View metadata, citation and similar papers at core.ac.uk
brought to you by CORE
provided by shahrekord university of medical scinces

International Journal of PharmTech Research
CODEN (USA): IJPRIF, ISSN: 0974-4304, ISSN(Online): 2455-9563
Vol.9, No.6, pp 261-273, 2016

Damage intensity of carvacrol on prostate cancer cells and its effects on molecular dynamic simulation of apoptotic factors

Javad Saffari Chaleshtori[1], Ehsan Heidari Soreshjani[2*], Fateme Reisi[3], Mohamad Amin Tabatabaiefar[4], Majid Asadi-Samani[5], Navid Zamanian[6], Mahmoud Bahmani[7]

[1]Clinical Biochemistry Research Center, Shahrekord University of Medical Sciences, Shahrekord, Iran
[2]Young Researchers and Elites Club, Islamic Azad University, Shahrekord Branch, Shahrekord, Iran
[3]Department of Biology, Faculty of Basic Sciences, Shahrekord Branch, Islamic Azad University, Shahrekord, Iran
[4]Department of Genetics and Molecular Biology, School of Medicine, Isfahan University of Medical Sciences, Isfahan, Iran
[5]Medical Plants Research Center, Shahrekord University of Medical Sciences, Shahrekord, Iran
[6]Computer Engineer, Iran Technical & Vocational Training Organization, Shahrekord, Iran
[7]Razi Herbal Medicines Research Center, Lorestan University of Medical Sciences, Khorramabad, Iran

Abstract: Prostate cancer is one of the most dangerous diseases in men worldwide. The apoptotic factors such as BID, BIM and APAF1 have a main role in inducing apoptotic pathways. Some of the compounds can active this apoptotic factors. In this study, this notion was investigated by the use of the comet assay technique and molecular dynamics simulations. In the comet assay technique, different concentrations including 130, 230, and 360 µM of carvacrol were selected according to IC50 using MTT assay on the cell line DU145. Then, alkaline electrophoresis was performed and 100 comet pictures were analyzed using CASP software. Data were analyzed by SPSS statistical software and also using molecular dynamic simulations, wherein protein and carvacrol were studied, thus avoiding the necessity for quantum mechanical calculations. Molecular dynamic simulations were carried out using carvacrol in a fully hydrated simulation box with a protein (Bak, Bax, Bim, Apaf1, Bid and P38). The IC50 for carvacrol was determined at 360 µM by MTT test. Rate of tail to head in alkaline electrophoresis at 130, 230, and 360 µM of carvacrol concentrations were 13.8±0.3, 40.6±0.3, and 47.6±0.5 percent, respectively. Statistical analysis of the molecular dynamics and calculated potential energy, radius of gyration (Rg), temperature, root mean square fluctuation (RMSF) and root mean square deviation (RMSD) indicated that carvacrol affected protein which stimulated the apoptosis cascade. Therefore, both experimental and theoretical results demonstrate carvacrol directly affects factors initiating apoptosis.
Keywords: Simulation, Carvacrol, DU145 cell line, Prostate cancer, Comet assay.

Introduction

Cancer is the most complex disease tightly associated with abnormal intracellular signal transduction system. Prostate cancer is one of the most prevalent cancers among men worldwide. It ranks second most frequent cancer among men in the United States [1]. The frequency of the cancer is growing in Asian countries. The role of apoptosis, the process of programmed cell death,has been studied and is crucialin cancer treatment [2].Major factors that initiate the apoptotic cascade in the cell include: Bak, Bax, Apaf1, Bim, Bid and P38.Bax and Bak can form hetero- or homodimerproteins and serve as anti- or pro-apoptotic regulators [3, 4].

Activation of Bax/Bak causes mitochondrial outer membrane permeabilization (MOMP), which, in turn, is necessary for the release of apoptogenic factors such as cytochrome C. Thence, the effectors caspase-3 and -7, involved in the intrinsic mitochondrial apoptotic pathway, become active. This activation requires the action of a subgroup of the Bcl-2 family, called the BH3-only proteins, which either directly activate Bax/Bak (such as tBid, Bim or Puma) or bind to Bcl- 2-like survival factors to release it from prebound Bax/Bak for oligomerization and MOMP induction [5].Bid (BH3 Interacting domain Death agonist) is a CASP-8 specific substrate in the Fas apoptotic signaling pathway which mediates mitochondrial damage induced by CASP-8[6]. Bim (BCL2 Interacting Protein) is an apoptotic factor and a regulator of the cell growth [7]. Apaf1 (Apoptotic Protease Activating Factor1) is also a major player in apoptosis. It is involved in the activation of the procaspase-9 and maintenance of the enzymatic activity of processed caspase-9. Therefore, it induces a cascade of proteolytic events culminated in the cell apoptosis [8]. P38 protein kinase is acellular stress-activated MAP kinase. Cellular stress can cause apoptosis which is often initiated through the mitochondria. The Bcl-2 protein family can regulator this process through modulating the membrane potential and the function of mitochondria [9].

Herbal ingredients such as polyphenolic compounds and anti-oxidants have been shown to prevent cancer [10]. In this regard, much effort has been made to characterize plant compounds with sufficient anti-cancer effect without inducing damage on normal cells [11]. Carvacrol (2-methyl-5-(1- methylethyl)-phenol) is a natural member of monoterpene phenol present in the volatile oils of *Thymus vulgaris*, *Carum copticum*, and some other medicinal plants. Carvacrol is one of this compounds that exist abundance in green tea and cumin too [12]. It has been shown that carvacrol increases the rate of apoptosis in cancer cells including hepatocellular carcinoma [13, 14]. Carvacrol has been shown to exert anti-proliferative effects on many cancers including non-small cell lung cancer cells (A549) chronic myeloid leukemia cells (K562, Hep-2 cells), murine B16 melanoma cells and human metastatic breast cancer cells (MDA-MB231) and many others [10, 15]. It is one of the powerful antioxidants that can induce apoptosis in chronic myeloid leukemia and breast cancer and prevent their growth [16].

The comet assay technique is an alkaline electrophoresis that can rapidly and easily detect the amount of DNA damage in the cell [17]. Docking is the field of molecular modeling which predicts the preferred orientation of molecules when bound to each other to form a stable complex and could be used to predict the strength of signal. Furthermore, the relative orientation of the two interacting partners may affect the type of signal produced [18]. Molecular dynamics (MD) is a computer simulation of physical movements of atoms and molecules in the context of N-body simulation. The trajectories of atoms and molecules are determined by solving the Newton's equations of motion for a system of interrelating particles, where interatomic potentials or molecular mechanics force fields are used to define forces between the particles and potential energy [19, 20]. Due to the positive effects of carvacrol on apoptosis pathway, the present study was launched to evaluate the effect of carvacrol on the activity of Bak, Bax, Bim, Bid Apaf1 andP38using molecular dynamic simulation also the effect of carvacrol on DNA damage and cell death in prostate cancer cell line, DU145,was performed by the comet assay technique.

Materials and Methods

Cell Culture

The prostate cancer cell lines, Du145, were supplied by Iran Pasteur Institute. The cells were moved to 75ml tissue culture flasks (TPP Switzerland) and cultured in 15ml RPMI supplemented with 10 % FBS, 2 mM glutamine, and 1% (100 µg/mL/100 U/mL) penicillin/streptomycin antibiotics and were incubated for 24 h at 37ºC in a CO2 incubator.

MTT assay

Cells were seeded in a multi-well plate including 2 mL at 150 × 10^3 cells/mL in RPMI medium supplemented with 10% FBS, 2 mM glutamine, and 1% (100 µg/mL/100 U/mL) penicillin/ streptomycin antibiotics and were incubated for 24 h at 37 ºC in a CO2 incubator. The livability of cells in various concentration of carvacrol was detected by MTT [3-(4,5-dimethylthiazol-2-yl)-2,5-diphenyl-terazolium bromide] (BIO-IDEA) assay kit and the P_{50}determined. Three concentrations below the P_{50}were chosen for the comet assay.

Comet assay

For positive control in comet assay we used 30µM H_2O_2treatment. Cells were seeded in a multi-well plate including 2 mL at 150 × 10^3 cells/mL in RPMI. Cells were cultured in a medium supplemented with 10 % FBS, 2 mM glutamine, and 1 % (100 µg/mL/100 U/mL) penicillin/streptomycin antibiotics and were incubated for 24 h at 37ºC in a CO2 incubator. DU145 cell line treatment was done to induce DNA damage according to a method previously described [21].

The alkaline comet assay was performed following standard protocol described by McKelvey-Martin et al. with some modifications [17].All slides were washed with methanol and heated to remove the proteins. Dakin microscope slides were covered with 250–300 µL of 0.1 % normal melting point agarose (Gibco, Carlsbad, Ca, USA) prepared in PBS at 50ºC and allowed to be fully frosted. To solidify agarose, a coverslip was placed on top and the slide was kept on ice. Each pellet of cells (prepared as described above) was re-suspended in 80 µL of low melting point agarose at 37ºC. After gently removing the coverslip, the cell suspension was quickly pipetted onto the first agarose layer and the coverslip was replaced on top and the slide left on ice to solidify the agarose. The coverslip was gently removed and the third layer of 250–300 µL of 0.1 % normal melting point agarose was added. After removing the coverslips, slides were quickly immersed in freshly prepared cold lysis solution (2.5 M NaCl, 100 mM Na2EDTA, 10 mM Tris, pH 10, with 1 % Triton X-100 and DMSO 10 % added just before use) for 12 h at 4ºC. After lysis, the slides were drained and placed side by side in a horizontal gel electrophoresis tank. The tank was filled with fresh and cold electrophoresis buffer (300 mM NaOH, 1mMNa2EDTA, pH>13) to a level of approximately 0.25 cm above the slides. The slides were left in the alkaline buffer for 30 min to allow for DNA unwinding. Electrophoresis was performed at 25 V (0.66 V/cm) and 300 mA for 30 min at room temperature. After electrophoresis, the slides were drained and placed on a tray and flooded slowly with three stages of neutralization buffer (0.4 M Tris, pH 7.5) for 5 min to remove alkali and detergents. All slides were once washed with ethanol 95 % for 5 min. Slides were drained and stained with 2 µg/mL ethidium bromide and left in a humidified chamber at 4ºC prior to analysis. All slides were prepared under UV light and duplicate slides for each treatment were prepared. The parameters of alkaline comet assay include head area, tail area, head DNA, tail DNA, tail length, comet length, and tail moment of positive control and sample cells were evaluated by CaspLab (Comet Assay Software Project) software version 1.0.0.

Statistical analysis

Each experiment was performed at least three times. Data of all experiments were collected in Statistics programs for the Social Sciences software, version 17 (SPSS, Inc., Chicago, IL, USA). The alkaline comet assay parameters were evaluated by CaspLab software version 1.0.0 and the within groups variance was calculated by ANOVA (Analysis of variance) test. The 0.05 % (5 %) was considered as statistically significant.

Structural studies of protein and ligand

The three-dimensional (3D) structure of Apaf1, Bak, Bax, Bid, Bimand P38 was obtained from protein database PDB. The PDB ID of the selected proteins is given in table 1. Carvacrol ($C_{10}H_{12}OH$) (Figure 1) was obtained with CID numbers 10364from NCBI Pub Chem. The ligands were obtained in SDF format and converted into PDB using Spdbv. Then all of the missing atoms of Bak, Bax, Bid, Bim, Apaf1 and P38 were modified with Swiss-pdb Viewer 4.1.0.

Table 1: Summery of simulation.

Number of ionCl-	Number of ion Na+	Times simulation (ns)	Distance between the protein and the edge of the box(nm)	Number of water	PDB ID	Protein	Simulation
22	22	10	2.3*2.9*2.07	4270	2YGS	Apafl	1
25	23	10	3.8*3.8*2.7	9600	2BID	Bid	2
21	21	10	3.6*3.6*2.5	8262	3FDL	Bim	3
8	8	10	3.8*3.8*2.7	3205	2YV6	Bak	4
25	24	10	3.8*3.8*2.7	9629	1F16	Bax	5
29	29	10	4.14*4.14*2.93	11634	1A9U	P38	6

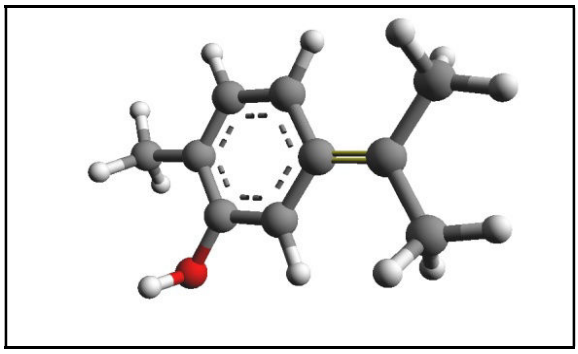

Figure 1: The structure of carvacrol

Docking Analysis

For docking the carvacrol into the binding site of the ligands and estimating the binding affinity of the complexes, the AutoDock 4.2 software was used [22]. Autodock needs receptor and ligand representations in a file format called pdbqt which is a modified protein data bank. The search algorithm was used in the AutoGrid program based on defined all molecules active and generated the grid parameter files. Scoring algorithm in the Autodock program was used for binding conformation of ligand. Using Lamarckian genetic algorithm (LGA), hundred runs of docking were performed. Ligplot plus was used to analyze docking poses for Hydrogen bonding and hydrophobic bonding.

Molecular dynamic simulation

The molecular dynamic simulation was performed with GROMACS 4.5.7 package with the G43a1 force field [23].The calculations were carried out using the structure of the apoptosis components and carvacrol downloaded from the Protein Data Bank (http://www.rcsb.org). The protein and ligands was embedded into a box containing the SPC model water (24). The specification boxes and the number of water and ions are shown in table 1. Although more complex water models are nowadays frequently used in the simulation of proteins, we chose to use the SPC, as it was found to give better results for simulations of solutes in water when compared to more sophisticated water models [25], especially at interfaces (26).Simulation was done with the specified number from Na+ and Cl− ions (Table 1), corresponding to a salt concentration of ∼140mM, which were added to the system by replacing the water molecules in random positions. Before the dynamics simulation, internal constraints were relaxed by energy minimization. After the minimization, an MD equilibration run was performed under position restraints for 20 ps. A 10-ns-long production MD run was performed after the equilibration. During the MD run, the LINCS algorithm [27].Was applied to constrain the lengths of hydrogen-containing bonds; the water molecules were restrained using the SETTLE algorithm [28]. The time step for the simulation was 2 fs. The simulations were run under NPT conditions, using Berendsen's coupling algorithm [29] to keep the temperature and the pressure constant (P = 1 bar, τP = 0.5 ps; T = 300° K; τT = 0.1 ps). Van der Waals forces were treated using a cutoff of 12 Å. Long-range electrostatic forces were treated using the particle mesh Ewald method [30].The coordinates were saved every 0.5 ps.

Results

The MTT assay results:

The various concentrations (between 0 - 1000µM) of carvacrol were used on prostate cancer cells line DU145. The IC_{50} of these concentrations was determined to be about 360µMusingthe MTT assay. High concentrations of carvacrol can cause cell death (Figure 2). In lower concentrations such as 360µM of carvacrol, 50 percent of cells were alive. In lower concentrations such as 230 and 130 µM of carvacrol above 60 percent of cells survived.

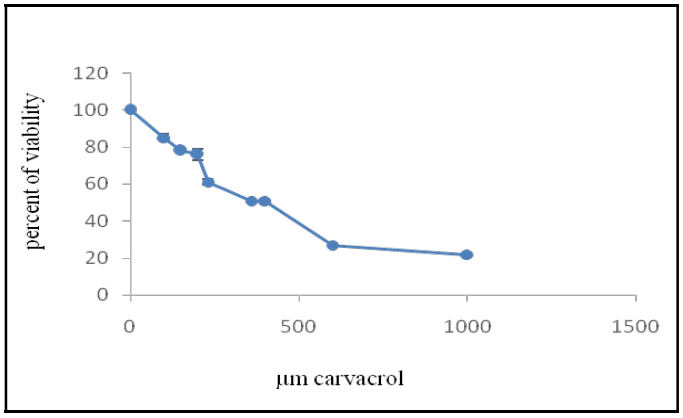

Figure 2: Percentage of viability in the various concentrations of carvacrol on prostate cancer cell line DU145. In concentrations of 230 and 130 µM of carvacrol over 60 percent of cells were alive.

The comet assay results:

The details of alkaline comet assay analysis on prostate cancer cell line DU145 with various concentrations of carvacrol (130, 230 and 360 µM carvacrol) is shown in Table 2. In this study, we used prostate cancer cell line DU145 treated with 50 µM of H_2O_2 as positive control and prostate cancer cell line DU145 without treatment (0 µM of carvacrol) as negative control. Rate of tail comet to head comet is increased in parallel with increasing carvacrol concentration. A comparative chart of percent of DNA in the comet tail to comet head in Du145 cell line treated with various concentrations of carvacrol is shown in figures 3, 4 and 5.

Table 2: The details of alkaline comet assay analysis on prostate cancer cell line DU145 with various concentrations of Carvacrol (130, 230 and 360 µM) positive control with H_2O_2 50 µM and negative control without treatment (0 µM of Carvacrol).

Parameter	n	Control -	130	230	360	Control +
Head Area	100	349.5±52.9	11039.3±126.5	952.7±0.05	1150.2±45	356.9±14.2
Tail Area	100	41.2±18.1	4329.7±73.8	1562.3±1901	2136.2±91	1821.4±15.3
Head DNA	100	35.4±5.3	710.1±6.7	130.2±0.6	85.2±4.5	27.1±13.0
Tail DNA	100	1.0±0.5	114.1±2.4	89.2±0.6	81.7±4.8	68.1±17.5
Head DNA%	100	97.2±1.2	86.1±0.3	59.4±0.3	52.4±0.6	27.2±5.7
Tail DNA%	100	2.8±1.2	13.8±0.3	40.6±0.3	47.6±0.5	72.8±5.7
Head Radius	100	10.3±0.9	59.3±0.3	18.1±0.1	18.3±0.4	10.7±3.7
Tail Length	100	4.1±1.2	42.2±0.7	23.2±0.4	44.5±1.4	44.9±3.3
Comet Length	100	25.7±2.6	92.5±7.2	60.4±0.4	82.2±2.0	67.3±9.8
Head Mean X	100	1.1±0.2	86.2±1.3	29.1±0.4	42.5±1.4	32.6±3.0
Tail Mean X	100	349.5±3.2	136.9±1.3	54.3±0.1	69.9±2.1	356.9±3.4
Tail Moment	100	41.2±1.3	5.8±0.5	9.5±0.2	21. 9±0.8	1821.4±5.3
Olive Tail Moment	100	35.4±2.1	7.0±0.1	10.3±0.2	13.4±0.5	27.1±1.3

Head area: area of the comet head in pixels, Tail area: area of the comet tail in pixels, Head DNA: amount of DNA in the comet head, Tail DNA: amount of DNA in the comet tail, Head DNA%: percent of DNA in the comet head to comet tail, Tail DNA%: percent of DNA in the comet tail to comet head, Head Radius:

Radius of the comet head (in pixels), Tail Length: length of the comet tail measured from right border of head area to end of tail (in pixels), Comet length: length of the entire comet from left border of head area to end of tail (in pixels), Head Mean X: Center of gravity of DNA in the head (x coordinate), Tail Mean X: Center of gravity of DNA in the tail (x coordinate), Tail moment: tail DNA % x tail length [(percent of DNA in the tail) x (tail length)].

Figure 3: The result of alkaline comet assay analysis on prostate cancer cell line DU145 with various concentrations of Carvacrol (130, 230 and 360 µM). A: cell line DU145without treatment. B: cell line DU145 treated with 130 µM of carvacrol. C: cell line DU145 treated with 230 µM of carvacrol. D: cell line DU145 treated with 360 µM of carvacrol. E: cell line DU145 treated with 50 µM of H_2O_2

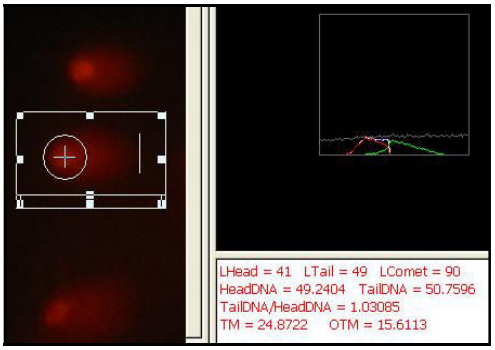

Figure 4: The analysis process includes percentage of DNA in the comet tail to comet head and other properties obtained by the Casp software.

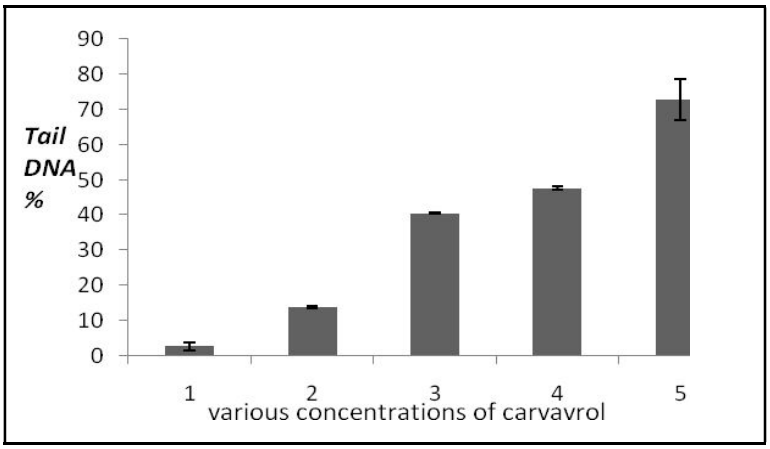

Figure 5: Percentage of DNA in the comet tail to comet head (Tail DNA%). 1: Du145 cell line without treatment (Control –). 2: Du145 cell line treated with 130 µM Carvacrol. 3: Du145 cell line treated with 230 µM Carvacrol. 4: Du145 cell line treated with 360 µM Carvacrol. 5: Du145 cell line treated with 50 µM H_2O_2(Control +)

Computational results:

Docking Analysis

To predict the appropriate interaction of carvacrol with Apaf1, Bak, Bax, Bid, Bim and P38 as receptors, the ligand molecules were docked with the target protein. Docking interaction details including binding energy (the sum of the intermolecular energy), the Torsional Energy, and the Internal energy are reported in table 3. A moderate binding was observed for the remaining ligands with binding energy in the range of -3 to -4 kcal/mol. The top hits were selected for further docking for the confirmation of binding pose and hydrogen bond interactions. Bak was of a high binding affinity with carvacrol with least binding affinity of 4.95Kcal/mol which confirmed an effective binding. We regarded carvacrol as a compound and further analyzed the binding poses in receptors structure. Analyzing hydrogen and hydrophobic bonding of carvacrol with each of the receptors are displayed in Table 3 and figures 6, 7, 8.

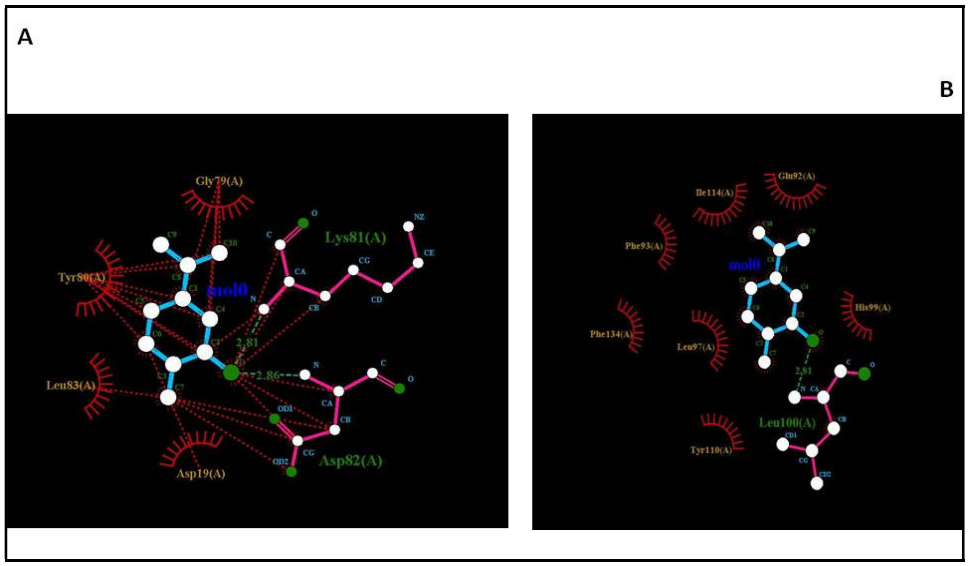

Figure 6: H-bond and hydrophobic analysis of docking poses by Ligplot plus tool for carvacrol ligands in Apaf1 (A) and Bak (B) domain after MD simulation.

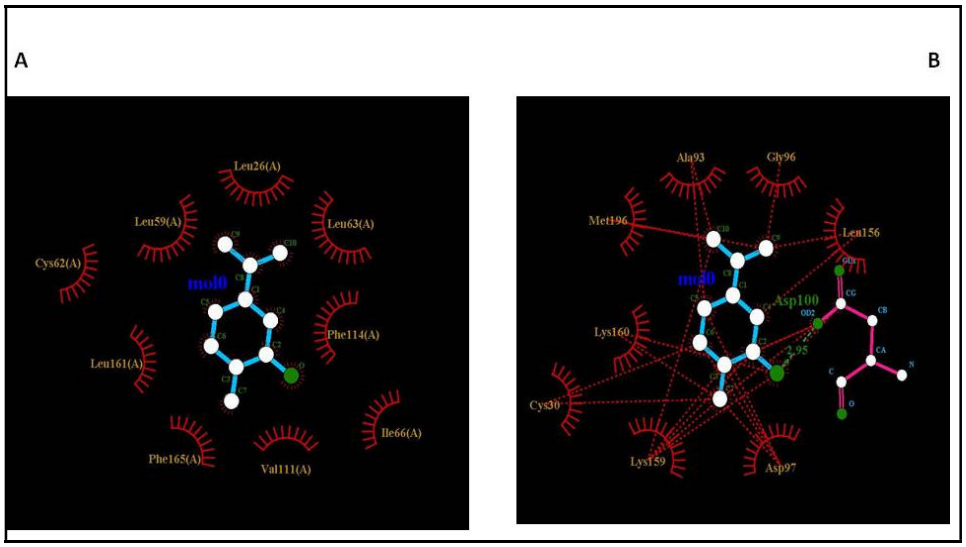

Figure 7: H-bond and hydrophobic analysis of docking poses by Ligplot plus tool for carvacrol ligands in Bax (A) and Bid (B) domain after MD simulation.

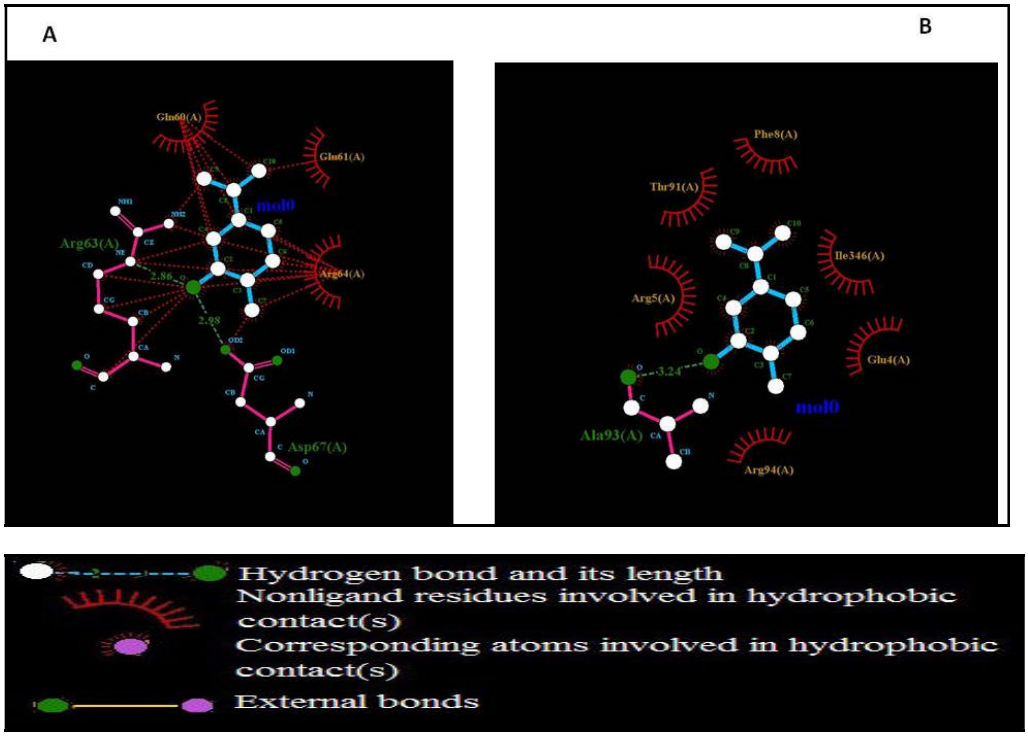

Figure 8: H-bond and hydrophobic analysis of docking poses by Ligplot plus tool for carvacrol ligands in Bim (A) and P38 (B) domain after MD simulation.

Table 3: Docking results with interacting residues after 100 runs of docking.

Receptors		Bak	Bax	Bid	Bim	Apaf1	P38
Binding and Energy(kcal/mol)		-4.95	-4.39	-3.82	-3.98	-4.67	-4.30
Final Intermolecular energy (kcal/mol)		-5.22	-4.67	-4.42	-4.57	-5.26	-4.58
Hydrogen bond (KJ/ mol)		-5.15	-4.66	-4.19	-4.32	-5.14	-4.56
Total Internalenergy (KJ/mol)		-0.12	0.12	-0.13	-0.13	-0.15	-0.12
Estimated Inhibition Constant, (KJ/micromolar)		236.66	601.41	1580	1220	378.66	699.44
RMSD from reference structure (A)		15.995	7.048	21.664	30.426	13.235	33.878
Interaction bonds	Hydrogen-Bonding	Leu100	-	Gly96, Ala93, Met196, Lys160, Cys30, Lys159, Asp97, Leu156, Asp100	Gln60, Glu61, Arg64, Arg63, Asp67	Gly79, Tyr80, Leu93, Asp19, Asp82, Lys81	Ala93
	Hydrophobic-Bonding	His99, Glu92, Ile114,Phe93, Phe134,	Val111, Ile66, Phe114, Leu63, Leu26, Leu59, Cys62, Leu161, PHe165	Gly96, Ala93, Met196, Lys160, Cys30, Lys159, Asp97, Leu156	Gln60, Glu61, Arg64	Gly79, Tyr80, Leu93, Asp19	Arg94, Glu4, Ile346, Phe8, Thr91, Arg5

Molecular dynamic simulation (MD) Analysis*:* The stability of the protein (bak, bid, bim, p38, bax, apaf1) during the simulation was evaluated by the root mean square deviation (RMSD) of protein relative to the starting structure. As documented in Figure 9, the RMSD of protein in the presence of carvacrol was steady over time, exhibiting some fluctuations that reached maximal values of 0.1-0.3 nm (except for the Bid and Bax protein) in the simulation. The RMSD of proteins represent the equilibration of all the system after about 8 ns of simulations. This consistency dictates that the protein was stable under the simulation conditions. The kinetic and potential energies fluctuated in equal and opposite directions in all phases during MD simulation (Table 4).

Table 4: The average RMSD, RMSF, Rg, kinetic, Temperature, average of distance center between of protein (Bak, Bid, Bim, Bax, Apaf1 and P38) and Carvacrol and potential energy during the last 8 ns of 10 ns MD simulation of protein (Bak, Bid, Bim, Bax, Apaf1 and P38) in the presences of Carvacrol.

Proteins / Variables	Apaf1	Bid	Bim	Bak	Bax	P38
A	1.16±0.007	1.63±0.01	1.19±0.004	1.45±0.007	1.55±0.01	2.15±0.01
B	299.5±3.29	300±1.68	299±2	300.4±2.8	299.8±1.99	299.7±1.8
C	35125±394.08	78979±443	64977±469	29565±284	784.9±556	99320±614
D	-199397±401.04	-445225±771	-372914±675	-156528±492	-440030±651	-548123±579
E	0.90±0.08	0.21±0.12	0.11±0.03	0.14±0.07	0.177±0.106	0.17±0.07
F	0.19±0.01	0.81±0.03	0.25±0.01	0.32±0.02	0.54±0.02	0.32±0.02
G	1.39±0.05	2.64±0.37	1.43±0.07	1.43±0.06	0.80±.08	2.7±0.12

A: Rg(nm); B: Temperature(K); C: Kinetic; D: Potential(KJ/mol); E: RMSF(nm); F: RMSD(nm); G: Distance center between protein and ligand(nm).

Table 4 shows the results of average of the potential energy, kinetic, radius of gyration (Rg), temperature, average of distance center between protein (Bak, Bid, Bim, Bax, Apaf1 and P38) and ligand, root mean square deviation (RMSD) of protein (Bak, Bid, Bim, Bax, Apaf1 and P38), root mean square fluctuation (RMSF) of protein (Bak, Bid, Bim, Bax, Apaf1 and P38) relative to initial positions during the last 8 ns of 10 ns MD simulation. Fluctuate of radius of gyration (Rg) of protein (Bak, Bid, Bim, Bax, Apaf1 and P38) in presence of carvacrol during the last 8 ns of simulation show carvacrol does change volume and three dimensional structures of proteins. Variations in potential and temperature during the last 8 ns of MD simulation are small (Table 4). These facts show the low potential energy during MD simulations and indicate the simulation times were sufficient and those simulations were stable under simulation conditions and simulations converge and also thermal equilibrium in the systems. The average of distance center between carvacrol and each protein during the last 8 ns MD simulation were represented in table 4. Average distance center at last 8 ns shows that value and the variations are therefore carvacrol more effect on these three molecules initiate apoptosis Bim, Bak and Bax. Also the results of average of root mean square fluctuation (RMSF) of protein (Bak, Bid, Bim, Bax, Apaf1 and P38) in presence of carvacrol were represented in table 4. These results show flexibility of protein Bim are more than in presence of carvacrol, whereas docking results showed that carvacrol more effective on protein. The result of the simulation is unlike the results of docking and this is due to dynamics and Brownian motion in simulation.

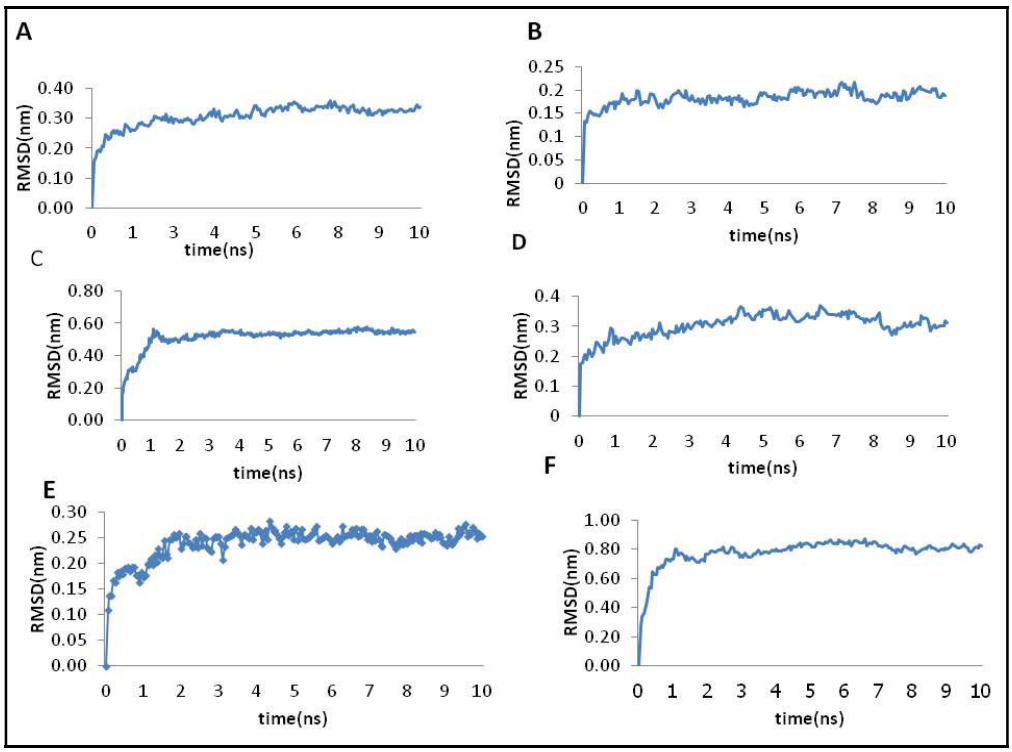

Figure 9: Root mean square deviation (RMSD) of protein Bak(A), Apaf1(B), Bax(C), P38(D),Bim(E) and Bid (F) during 10 ns MD simulation in the presence of different cation ions.

Discussion

According to studies on plants extracted compounds, obvious that they are very effective on induced the cell death in cancer cells line [31]. Zlotogorskiet al. in 2013 shown that poly phenolic compounds of green tea have antioxidant effects so can induce the apoptosis in head and neck cancers [32]. Carvacrol is one of the most important antioxidant compounds present in several plants consumed routinely in our diet. Carvacrol can induce apoptosis in several cancer studies [33, 34]. Hottaet al. in 2010 studied on thymol and carvacrol demonstrated that these compounds activate the many enzymes that are in apoptosis pathway too [35]. Yin et al. shown that carvacrol can die HepG2 cells via activation apoptosis by phosphorylation and dephosphorylation the apoptosis factors such as MAPK and ERK1/2.Anti-proliferative and pro-apoptotic effect of carvacrol on human hepatocellular carcinoma cell line HepG-2 [34]. Based on our results as well as those obtained by others using the comet assay various concentrations of carvacrol can have different effects on prostate cancer cells. In cells without carvacrol treatment (negative control) for 100 cells analyzed with the Casp software, 2.8±1.2percentof DNA was found to be in the comet tail to comet head. In cells treated with 130 µM of carvacrol we saw that Tail DNA% was 13.8±0.3 representing the cells with low damage in their genomes. Although 130 µM of carvacrol is lower than theIC_{50} obtained in MTT assay. In concentration of 230 µM which is closer to the IC_{50}, Tail DNA% was 40.6±0.3 that shows a higher damage in the cell genome. But in IC_{50} concentration and 360µM carvacrol tail DNA% was 47.6±0. The figure is comparable to the positive control treated with 50 µM H2O2, very close to the samples treated with230 µM carvacrol. The result reveals that carvacrol of 230 µM concentration can be better than the IC_{50} concentration as it is the minimum concentration of carvacrol which induces minimal damage to the normal cells.

Carvacrol was docked to Bak, Bid, Bim, Bax, Apaf1 and P38 proteins using autodock 4.0. The results shows that carvacrol strongly binds to Bak, Apaf1 and Bax ligands and their binding energies were found to be ΔG -4.95, -4.67, -4.39 (Kcal/mole), respectively.

The molecular dynamics simulation study was performed to compare the stability of the docked complex. The results showed that carvacrol causes apoptotic factors to initiate apoptosis (Bim>Bak>Bax> Bid). It also affects the apoptotic protease activating factor 1 and P38 mitogen activated protein kinases (Apaf1> P38).

Medicinal plants through their active ingredients have a good therapeutic effect of diseases (36-46). Carvacrol has an important role in direct activation of apoptotic molecules to initiate the apoptosis process.

Acknowledgments

We would like to thank head and deputy of research of Islamic Azad University of Shahrekord branch and Deputy of Research Medical Sciences Shahrekord in Iran for their sincere support**.**

References

1. Jemal A, Siegel R, Ward E, Hao Y, Xu J, Thun MJ. Cancer statistics, 2009. CA Cancer J Clin. 2009; 59 (4): 225-249.
2. Wong RS. Apoptosis in cancer: from pathogenesis to treatment. J ExpClin Cancer Res. 2011; 26: 30: 87.
3. Chittenden T, Harrington EA, O'Connor R, Flemington C, Lutz RJ, Evan GI, Guild BC. Induction of apoptosis by the Bcl-2 homologue Bak. Nature. 1995; 374 (6524): 733-7336.
4. Oltvai ZN, Milliman CL, Korsmeyer SJ. Bcl-2 heterodimerizes in vivo with a conserved homolog, Bax, that accelerates programmed cell death. Cell. 1993; 74(4):609-19.
5. Papaianni E, El Maadidi S, Schejtman A, Neumann S, Maurer U, Marino-Merlo F, Mastino A, Borner C. Phylogenetically Distant Viruses Use the Same BH3-Only Protein Puma to Trigger Bax/Bak-Dependent Apoptosis of Infected Mouse and Human Cells. PLoS One. 2015; 10(6): e0126645.
6. Li H, Zhu H, Xu CJ, Yuan J. Cleavage of BID by caspase 8 mediates the mitochondrial damage in the Fas pathway of apoptosis. Cell. 1998; 94(4):491-501.
7. O'Connor L, Strasser A, O'Reilly LA, Hausmann G, Adams JM, Cory S, Huang DC. Bim: a novel member of the Bcl-2 family that promotes apoptosis. EMBO J. 1998; 17(2): 384-95.
8. Bao Q, Lu W, Rabinowitz JD, Shi Y. Calcium blocks formation of apoptosome by preventing nucleotide exchange in Apaf-1. Mol Cell. 2007; 25(2):181-192.
9. Cai B, Chang SH, Becker EB, Bonni A, Xia Z. p38 MAP kinase mediates apoptosis through phosphorylation of BimEL at Ser-65. J Biol Chem. 2006; 281 (35): 25215-25222.
10. Lammer J, Malagari K, Vogl T, Pilleul F, Denys A, Watkinson A, Pitton M, Sergent G, Pfammatter T, Terraz S, Benhamou Y, Avajon Y, Gruenberger T, Pomoni M, Langenberger H, Schuchmann M, Dumortier J, Mueller C, Chevallier P, Lencioni R; PRECISION V Investigators. Prospective randomized study of doxorubicin-eluting-bead embolization in the treatment of hepatocellular carcinoma: results of the PRECISION V study. CardiovascInterventRadiol. 2010; 33(1):41-52.
11. Singh RP, Dhanalakshmi S, Agarwal R. Phytochemicals as cell cycle modulators: a less toxic approach in halting human cancers, Cell Cycle. 2002; 1(3): 56–161.
12. Uyanoglu M, Canbek M, Aral E, Husnu Can Baser K. Effects of Carvacrol upon the liver of rats undergoing partial hepatectomy. Phytomedicine. 2008; 15(3): 226-229.
13. Lampronti I, Saab AM, Gambari R. Antiproliferative activity of essential oils derived from plants belonging to the Magnoliophyta division. Int J Oncol. 2006; 29(4): 989-995.
14. Kiskó G, Roller S. Carvacrol and p-cymene inactivate Escherichia coli O157:H7 in apple juice. BMC Microbiol. 2005; 5: 36.
15. Koparal AT, Zeytinoglu M. Effects of Carvacrol on a Human Non-Small Cell Lung Cancer (NSCLC) Cell Line, A549. Cytotechnology. 2003; 43(1-3):149-54.
16. Arunasree KM. Anti-proliferative effects of Carvacrol on a human metastatic breast cancer cell line, MDA-MB 231. Phytomedicine. 2010; 17(8-9): 581-588.
17. McKelvey-Martin VJ, Ho ET, McKeown SR, Johnston SR, McCarthy PJ, Rajab NF, Downes CS. Emerging applications of the single cell gel electrophoresis (Comet) assay. I. Management of invasive transitional cell human bladder carcinoma. II. Fluorescent in situ hybridization Comets for the identification of damaged and repaired DNA sequences in individual cells. Mutagenesis, 1998; 13(1):1-8.
18. Lengauer T, Rarey M. Computational methods for biomolecular docking. CurrOpinStruct Biol. 1996; 6 (3): 402–406**.**
19. Alder, BJ,Wainwright TE. Studies in Molecular Dynamics. I. General Method. J Chem Phys. 1959; 31 (2): 459.

20. Rahman. A. Correlations in the Motion of Atoms in Liquid Argon". Physical Review. 1964; 136 (2A): A405–A411.
21. Benhusein GM, Mutch E, Aburawi S, Williams FM. Genotoxic effect induced by hydrogen peroxide in human hepatoma cells using comet assay. Libyan J Med. 2010; 13: 5.
22. Guex N, Peitsch MC. SWISS-MODEL and the Swiss-PdbViewer: an environment for comparative protein modeling. Electrophoresis 1997; 18 (15): 2714-23.
23. Project E, Nachliel E, Gutman M. Force field-dependent structural divergence revealed during long time simulations of Calbindin d9k. J Comput Chem. 2010; 31(9):1864-1872.
24. Berendsen HJC, Postma JPM, van Gunsteren WF, Hermans J. Interaction models for water in relation to protein hydration. Nature. 1969; 224: 175–177.
25. Van der Spoel D, Berendsen HJ. Molecular dynamics simulations of Leu-enkephalin in water and DMSO. Biophys J. 1997; 72(5): 2032-2041.
26. Tieleman DP, Berendsen HJC. Molecular dynamics simulations of a fully hydrated dipalmitoylphosphatidylcholine bilayer with different macroscopic boundary conditions and parameters. J Chem Phys. 1996; 105: 4871–4880.
27. Hess B, Bekker H, Berendsen HJC, Fraaije JGEM. LINCS: a linear constraint solver for molecular simulations. J Comput Chem. 1997; 18: 1463–1472.
28. Miyamoto S, Kollman PA. SETTLE: an analytical version of the SHAKE and RATTLE algorithms for rigid water models. J Comput Chem. 1992; 13: 952–962.
29. Berendsen HJC, Postma JPM, DiNola A, Haak JR. Molecular dynamics with coupling to an external bath. J Chem Phys. 1984; 81: 3684–3690.
30. Darden T, York D, Pedersen L. Particle mesh Ewald: an N-log (N) method for Ewald sums in large systems. J Chem Phys. 1993; 98: 10089–10092.
31. Zu Y, Yu H, Liang L, Fu Y, Efferth T, Liu X, Wu N. Activities of ten essential oils towards Propionibacterium acnes and PC-3, A-549 and MCF-7 cancer cells. Molecules. 2010: 30; 15(5): 3200-3210.
32. Zlotogorski A, Dayan A, Dayan D, Chaushu G, Salo T, Vered M. Nutraceuticals as new treatment approaches for oral cancer: II. Green tea extracts and resveratrol. Oral Oncol. 2013; 49(6): 502-506.
33. UmayaSuganthi R, Manpal S. Biological and Pharmacological of actions Carvacrol and its effects on poultry: an updated review world journal of pharmacy and pharmaceutical. Sciences. 2013; 2(5): 3581-3595.
34. Yin QH, Yan FX, Zu XY, Wu YH, Wu XP, Liao MC, Deng SW, Yin LL, Zhuang YZ. Anti-proliferative and pro-apoptotic effect of carvacrol on human hepatocellular carcinoma cell line HepG-2. Cytotechnology. 2012; 64(1):43-51.
35. Hotta M, Nakata R, Katsukawa M, Hori K, Takahashi S, Inoue H. Carvacrol, a component of thyme oil, activates PPARalpha and gamma and suppresses COX-2 expression. J Lipid Res. 2010; 51(1): 132-139.
36. Nikfarjam M, Bahmani M, Naimi A. Native medicinal plants of Iran effective on Memory and Learning: A Review. International Journal of PharmTech Research, 2016, 9(5), 466-473.
37. Asadi-Samani M, Moradi MT, Bahmani M, Shahrani M. Antiviral medicinal plants of Iran: A Review of Ethnobotanical evidence. International Journal of PharmTech Research, 2016, 9(5), 427-434.
38. Moradi MT, Asadi-Samani M, Bahmani M. Hypotensive medicinal plants according to Ethnobotanical evidence of Iran: A Systematic Review. International Journal of PharmTech Research, 2016, 9(5), 416-426.
39. Moradi MT, Asadi-Samani M, Bahmani M, Shahrani M. Medicinal plants used for liver disorders based on the Ethnobotanical documents of Iran: A Review. International Journal of PharmTech Research 2016, 9(5), 407-415.
40. Bahaa El-Din Mekki, Hebat-Allah Hussien, Hanaa Salem. Role of Glutathione, Ascorbic Acid and α-Tocopherol in Alleviation of Drought Stress in Cotton Plants, International Journal of ChemTech Research, 2016, 8(4), 1573-1581.
41. Helmina Br. Sembiring, TonelBarus, Lamek Marpaung, Partomuan Simanjuntak. International Journal of PharmTech Research, 8(9), 24-30.
42. Kartini Zailanie, Hartati Kartikaningsih, Umi Kalsum, Yushinta AristinaSanjaya. Fucoxanthin Effects of Pure Sargassumfilipendula Extract Toward HeLa Cell Damage, International Journal of PharmTech Research, 2015, 8(3), 402-407.

43. Hashish Kh I, Rawia A Eid, Magda M Kandil, Azza AM Mazher. Study on Various Level of Salinity on Some Morphological and Chemical composition of gladiolus Plants by Foliar Spray with Glutathione and Thiamine, International Journal of ChemTech Research, 2015, 8(9), 334-341.
44. Mahmoud Khaled F, Azza A Amin, Effat I Seliem, Manal F Salama. Nano Capsulated Polyphenol Extracted from Oyster Mushroom (Pleurotusostreatus), Characterization and Stability Evaluation, International Journal of PharmTech Research, 2016, 9(3), 103-113.
45. Mervat Sh Sadak. Mitigation of drought stress on Fenugreek plant by foliar application of trehalose. International Journal of ChemTech Research, 2016, 9(2), 147-155.
46. Nadia Gad, Abdel-Moez MR. Effect of cobalt on growth and yield of fenugreek plants, International Journal of ChemTech Research, 2015, 8(11), 85-92.

*****